Article

Multi-Objective Optimization of the Setup of a Surfactant-Enhanced DNAPL Remediation

Jan Schaerlaekens, Jan Carmeliet, and Jan Feyen

Environ. Sci. Technol., **2005**, 39 (7), 2327-2333 • DOI: 10.1021/es049148z

Environ. Sci. Technol. **2005**, *39,* 2327−2333

Multi-Objective Optimization of the Setup of a Surfactant-Enhanced DNAPL Remediation

JAN SCHAERLAEKENS,*,† JAN CARMELIET,‡ AND JAN FEYEN†

Laboratory for Soil and Water Management, Katholieke Universiteit Leuven, V. Decosterstraat 102, B-3000 Leuven, Belgium, and Laboratory for Building Physics, Katholieke Universiteit Leuven, Kasteelpark Arenberg 51, B-3001 Heverlee, Belgium

Surfactant-enhanced aquifer remediation (SEAR) is widely considered a promising technique to remediate dense nonaqueous phase liquid (DNAPL) contaminations in-situ. The costs of a SEAR remediation are important and depend mostly on the setup of the remediation. Costs can be associated with the installation of injection and extraction wells, the required time of the remediation (and thus labor costs, lease of installations, and energy), the extracted water volume (the purification of the extracted water), and the injected surfactant amount. A cost-effective design of the remediation setup allows an optimal use of resources. In this work, a SEAR remediation was simulated for a hypothetical typical DNAPL contamination. A constrained multi-objective optimization of the model was applied to obtain a Pareto set of optimal remediation strategies with different weights for the two objectives of the remediation: (i) the maximal removal of DNAPL mass (ii) with a minimal total cost. A relatively sharp Pareto front was found, showing a considerable tradeoff between DNAPL removal and total remediation costs. These Pareto curves can help decision makers select an optimal remediation strategy in terms of cost and remediation efficiency depending on external constraints such as the available budget and obligatory remediation goals.

1. Introduction

Chlorinated compounds have been widely used in the metal industry, machine manufacturing, and the electronics industry for decades. As a result of accidents and spills, they have been released to the subsurface in large quantities. The occurrence of resulting dense nonaqueous phase liquid (DNAPL) contamination in the subsurface is one of the most challenging environmental problems in the industrialized world (*1*, *2*). Most DNAPL forming contaminants are toxic; hence many DNAPL contaminations lead to a risk for drinking water resources. Due to the special physical and chemical characteristics of DNAPLs (low aqueous solubility and high interfacial tensions with water), these contaminants are very difficult to remediate with classic in-situ remediation techniques such as pump-and-treat. These characteristics render the remediation of DNAPLs a difficult and costly business (*3*, *4*). Surfactant-enhanced aquifer remediation (SEAR) is one of the most promising techniques to increase the effectiveness of classic pump-and-treat remediations. The SEAR technique consists of the injection of a surfactant solution into the contaminated zone and the extraction of water, surfactants, and dissolved contaminants with subsequent treatment at the surface.

Experimental research on SEAR has been performed at different scales (column, scale-model, and field experiments). Brown et al. (*5*) described the results of a SEAR pilot test in Operational Unit 2 (OU2) of Hill Air Force Base in Utah. The DNAPLs consisted mainly of TCE, PCE, and TCA. The surfactant used was sodium dihexyl sulfosuccinaat (SDS) and this solution succeeded in removing 99% of the available DNAPL. The remediation was modeled with UTCHEM (*6*). Istok et al. (*7*) combined solubilization and mobilization for a "push−pull" remediation of TCE contamination. Other reports on mobilization experiments on a field scale can be found in refs *8*−*16*. The data resulting from the field-scale pilot test described by ref *19* were used for inversed modeling with the UTCHEM model.

Mathematical models for the description of surfactant-enhanced DNAPL remediation allow a better understanding of the observed phenomena and the possibility to extend the established knowledge to greater scales and more complex situations, and to conduct an economic evaluation prior to the implementation (*20*). Models enable a better design and management of field remediations and a reduction of possible risks. Models are increasingly used as a basis for managing and optimizing remediation problems. It is common sense that a remediation results in important costs. These costs originate from preliminary sampling and analyses, the installation of injection and extraction wells, the time that the remediation lasts (labor costs, leasing of machines, energy, etc.), the cost of the injected surfactant, and the cost of decontamination of the extracted water (*19*). A cost-effective optimization of the remediation technique is therefore required to minimize the total cost.

The design problem for remediations is a constrained, nonlinear, discontinuous, multi-objective optimization problem (*21*). Constrained because there exist physical and economical boundaries to remediation variables (e.g., the extraction rate is limited by the aquifer characteristics, the duration of the remediation is limited by the desires of the title holder). The nonlinear nature of these problems results from the nonlinear nature of most subsurface hydrologic and transport processes. The problem is discontinuous because particular remediation variables (e.g., the number of extraction wells) have a discontinuous nature. The multi-objective aspect of these problems is related to conflicting objectives one may encounter when designing a field site remediation (*19*, *21*, *22*), e.g., the requirement to minimize the total cost versus the desire to minimize the remaining contaminant mass in the subsurface.

This work focuses on the multi-variable multi-objective optimization of a hypothetical SEAR remediation of a DNAPL contamination. The main objective was to present a general "modus operandi" for giving a model-based economical background for the decision-making process and to evaluate the tradeoff between remediation targets and remediation costs. The altered remediation variables were pumping well setup (total number, configuration, and mutual distance of the injection and extraction wells), the injection and extraction pumping rates, the duration of the remediation steps, and the injected surfactant concentration. The two objectives were a minimal remediation cost and a maximal remediation

* Corresponding author phone: +32-486-21 59 61; fax: +32-16-32 97 60; e-mail jan.schaerlaekens@gmail.com.
† Laboratory for Soil and Water Management.
‡ Laboratory for Building Physics.

10.1021/es049148z CCC: $30.25
Published on Web 03/03/2005

result (i.e., minimal fraction of remaining DNAPL in the system).

2. Modeling

2.1. UTCHEM. The scenarios were modeled using the University of Texas Chemical Compositional Simulator (UTCHEM) model (*23*−*25*). UTCHEM is a 3-D, multiphase, and multicomponent finite differences model. It is able to model complex physical and chemical reactions, including the surfactant-enhanced solubilization and mobilization of DNAPLs. The simulator is able to incorporate multiple components (e.g., dissolved organics, surfactants) in multiple phases (e.g., aqueous phase, DNAPL). UTCHEM makes use of a solution scheme that is implicit in pressure and explicit in saturation and concentration (IMPESC). The version used for this work was UTCHEM 9.6 (2002), obtained from the University of Texas at Austin. DNAPL mobilization is modeled in UTCHEM by relating the residual DNAPL saturation and the relative permeability to the dimensionless trapping number (N_T) (*26*). This trapping number is a vector summation of the capillary number (N_{Ca}) and the Bond number (N_B), a measure for the ratio of viscous forces (= groundwater flow driven forces) to capillary forces and of buoyancy forces (caused by gravitation) to capillary forces, respectively. The definition for the trapping number is as follows:

$$N_T = \sqrt{(N_{Ca})^2 + 2N_{Ca}N_B \sin\theta + (N_B)^2} \quad (1)$$

$$N_{Ca} = \frac{q_a \mu_a}{\gamma_{n,a}} \quad (2)$$

$$N_B = \frac{\Delta\rho_{n,a} g k}{\gamma_{n,a}} \quad (3)$$

with θ (rad) being the angle between the water flow direction and the horizontal, q_a (L T^{-1}) being the Darcy flow, μ_a (M L^{-1} T^{-1}) being the dynamic viscosity, and $\gamma_{n,a}$ (M T^{-2}) being the interfacial tension between the NAPL and the aqueous phase; $\Delta\rho_{n,a}$ (M L^{-3}) is the difference in density between the DNAPL and water, g (L T^{-2}) is the acceleration due to gravity, and k (L^2) is the permeability.

In UTCHEM, the residual saturation is dependent on the trapping number as follows (*23*, *25*):

$$S_n^r = \min\left(S_n, S_n^{r,high} + \frac{S_n^{r,low} - S_n^{r,high}}{1 + T_n + N_T}\right) \quad (4)$$

where S_n^r (unitless) is the residual NAPL saturation, S_n (unitless) is the NAPL saturation, $S_n^{r,high}$ (unitless) and $S_n^{r,low}$ (unitless) are the input residual saturations at low and high trapping numbers, respectively, and T_n (unitless) is a positive input parameter based on the experimental observation of the relation between residual saturations and trapping number.

The endpoints k_n^{end} (unitless) and exponents n (unitless) in Brooks Corey relative permeability functions are computed as a linear interpolation (*23*, *25*) between the given input values at low and high trapping numbers ($k_n^{end,low}$, $k_n^{end,high}$, n^{low}, n^{high}) as follows:

$$k_n^{end} = k_n^{end,low} + \frac{S_n^{r,low} - S_n^r}{S_n^{r,low} - S_n^{r,high}}(k_n^{end,high} - k_n^{end,low}) \quad (5)$$

$$n = n^{low} + \frac{S_n^{r,low} - S_n^r}{S_n^{r,low} - S_n^{r,high}}(n^{high} - n^{low}) \quad (6)$$

The Huh (*27*) model (eq 7) quantifies the dependence of the interfacial tension (IFT) to the concentration, or

$$\gamma_{n,a}^{surf} = \gamma_{n,a}^{pure} e^{-aR} + \frac{cF}{R^2}(1 - e^{-aR^3}) \quad (7)$$

with $\gamma_{n,a}^{surf}$ (M T^{-2}) the IFT between NAPL and the aqueous phase in the presence of surfactants, $\gamma_{n,a}^{pure}$ (M T^{-2}) the IFT in pure water, R (unitless) a solubilization ratio (the ratio of volume of contaminant solubilized in the microemulsion phase to the volume of surfactant in this phase), and F (unitless) (*28*) a correction factor; a (unitless) and c (unitless) are empirical parameters.

TABLE 1. Aquifer Input Data

parameter		units
variance (ln(k))	0.51	mD[a]
mean (ln(k))	10.59	mD
horizontal correlation length (X, Y)	5.1	m
vertical correlation length (Z)	0.2	m

[a] 1 mD = 9.87 × 10^{-2} μm^2.

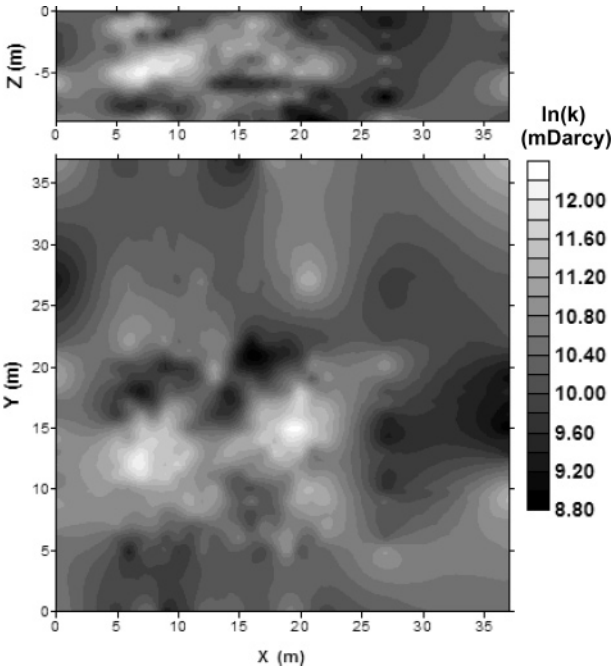

FIGURE 1. Aquifer permeability field (*XZ* at *Y* = 23 m and *XY* at *Z* = 5 m).

2.2. Simulation Setup. To study the remediation of a DNAPL spill, a base simulation scenario was defined describing a water-saturated aquifer. A log-normal-distributed three-dimensional permeability field with a spatial correlation structure was created as aquifer (*29*) using a Kraichnan random field generator (*30*). The domain has dimensions in the X−Y−Z-direction of, respectively, 47 by 47 by 10 m. The geostatistical parameters from the Borden aquifer as reported by Woodbury and Sudicky (*31*) are used as presented in Table 1.

This gives a permeability field as shown in Figure 1. The central part of the aquifer (7 by 7 by 5 m) contains a residual DNAPL. It is supposed that the central part of the domain has been saturated with DNAPL and then drained until the residual saturation was reached. A functional dependence of residual nonwetting phase saturation on capillary number (and thus on permeability) has been reported (*24*, *32*, *33*). The dependence is frequently observed to be log-linear. Hoag and Marley (*32*) reported a correlation of the following form:

$$S_n^{res} = -13.83 - 5.67\log(k) \quad R^2 = 0.76 \qquad (8)$$

where S_n^{res} (unitless) is the residual DNAPL saturation and k (cm^2) is the permeability.

The resulting initial saturation field is shown in Figure 2. In this way, a reproducible DNAPL contamination could be created with a result that is not too dependent on very local permeabilities. This avoids the necessity to create a set of initial spills, which would increase the computational problem. A surfactant with the properties of Faliten VL was used in all the simulations (*19*). Faliten is a mixture of vegetal oils and anionic and nonionic surfactants. It reduces the interfacial tension between TCE and water considerably in relatively small concentrations.

A series of nine scenarios with an increasing number of pumping wells (and a decreasing mutual distance) was selected. All nine scenarios have a pumping scheme where injection is supported by a simultaneous extraction in other points to facilitate the injection of the surfactant. The injection in a certain point is always followed by extraction in the same point, which should minimize the risk for remaining surfactant in the subsurface (push−pull pumping, (*7*)) since it can be supposed that the pathways for surfactant injection are the same as the pathways for surfactant extraction. The nine scenarios contain some popular setup schemes in environmental modeling: a single well setup (scenario 1), a dipole (scenario 2), a central well (5-spot pattern, scenario 5), line drives (scenarios 2, 6, 8), and alternating wells (scenarios 3, 7, 9). All patterns used have extraction wells neighboring injection wells at all time steps because the extraction facilitates the injection of the surfactant solution in neighboring injection wells. The injection and extraction rates are the same in all injection points and respective extraction points during the remediation. An overview of the nine modeled scenarios is given in Figure 3.

The applied remediation is as follows: depending on the followed scenario (*scen*) a certain number of injection and extraction wells is installed. In a first time step (t_1), the surfactant solution with concentration (c_{surf}) is injected in the initial injection points at rate q_{inj}, whereas water is extracted at rate (q_{extr}) in the initial extraction points to support surfactant transport. In a second time step (t_2), water is extracted in the initial injection points (now thus extraction points) at the extraction rate (q_{extr}).

From the description of the UTCHEM model it becomes apparent that the parameters that describe the behavior of interfacial tension (σ_{na}), residual DNAPL saturation (S_n), and trapping number (N_T) are the most important for describing mobilization. Since these parameters are difficult or even impossible to measure, they were obtained through inverse optimization making use of field experiment data by Schaerlaekens et al. (*19*). They executed a field-scale pilot test in which a Faliten VL surfactant solution was injected in the center of a TCE-contaminated aquifer and extracted after a period. TCE and surfactant concentrations were measured at different spatial points and were used in an inverse optimization with UTCHEM. A compilation of these parameters and other (measured) parameters from their experiments is provided in Table 2.

2.3. Optimization. UTCHEM was used in a dual-objective constrained minimization. When using two objectives, the minimization problem can be stated as

$$\min\{F_1(p), F_2(p)\},\ p \in P \qquad (9)$$

where $F_i(p)$, $i = 1, 2$ are the two objective functions calculated for a parameter set p. The minimization problem is constrained, which means that p is restricted to the feasible or economical reasonable parameter space P. Minimization is carried out using the SCE algorithm (*34*−*37*). This algorithm

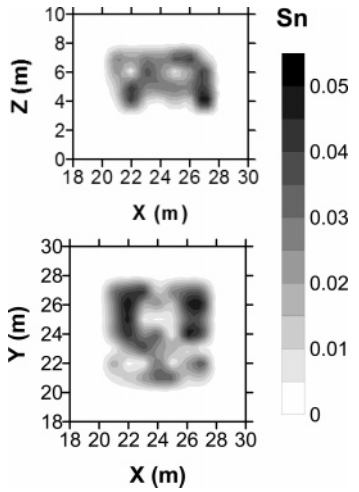

FIGURE 2. Initial residual DNAPL distribution (*XZ* at *Y* = 23 m, *XY* at *Z* = 5 m).

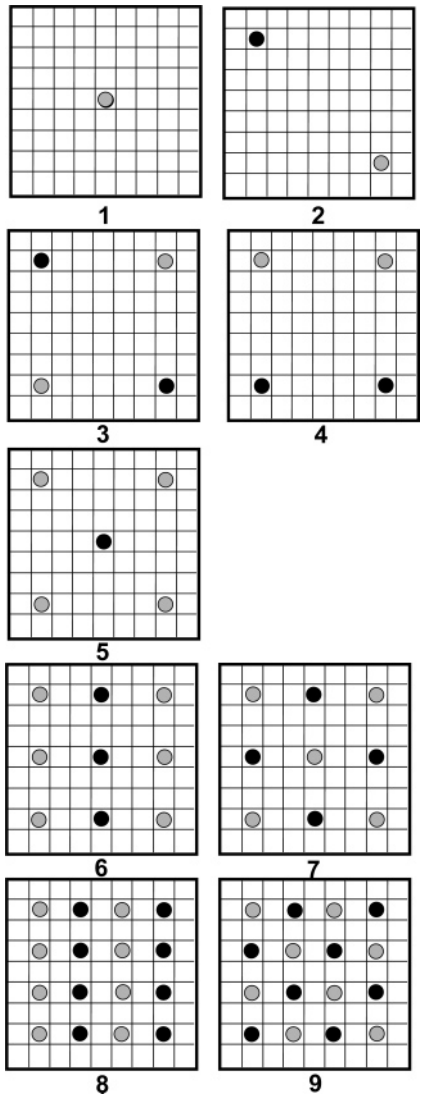

FIGURE 3. Central part of the aquifer with scenario setups and numbers with (grey dots) initial extraction wells and (black dots) initial injection wells (grid size = 1 m).

is a global search procedure based on the mechanics of natural selection and genetics, which combines an artificial survival of the fittest with genetic operators abstracted from nature. The algorithm carries out four steps. It starts with (i)

TABLE 2. Input Parameters for the UTCHEM Model

parameter	symbol	dimension	value
porosity	n		0.27
hydraulic gradient	ΔH		0.08
viscosity water	μ_a	cp	0.9
viscosity TCE	μ_n	cp	0.77
density water	ρ_a	g cm^{-3}	1
density TCE	ρ_n	g cm^{-3}	1.46
density Faliten VL	ρ_s	g cm^{-3}	1.001
critical micelle concentration Faliten VL	CMC	g cm^{-3}	0.05
salinity	S	meq/mL	0.0017
IFT TCE−pure water	γ	dyne cm^{-1}	29.4
molecular diffusion	D	cm^2 s^{-1}	9.3×10^{-6}
equilibrium solubility	S	mg L^{-1}	1100
Huh function value	a		0.81
capillary desaturation parameter	T_n		2.1×10^5
endpoint relative permeability at low N_{Ca}	$k_a^{end,low}$		0.388
endpoint relative permeability at high N_{Ca}	$k_a^{end,high}$		1
residual saturation at low N_{Ca}	$S_n^{r,low}$		0.35
residual saturation at high N_{Ca}	$S_n^{r,high}$		0.05
exponent at low N_{Ca}	n^{low}		2.16
exponent at high N_{Ca}	n^{high}		2.16

TABLE 3. Constraints of the Remediation Variables

remediation variable	lower constraint	upper constraint
summed extraction rate (m^3 d^{-1}) over all wells	0	100
summed injection rate (m^3 d^{-1}) over all wells	0	50
first remediation phase time extent (d) (central surfactant injection, boundary extraction)	0	70
second remediation phase time extent (d) (central extraction, boundary surfactant injection)	0	70
surfactant weight fraction (dimensionless)	0	0.05
scenario number (cf. Figure 3)	1	9

a random initialization, in which a number of n parameter sets are randomly chosen (within the range of constraints) and the associated objective functions are calculated. The random results are partitioned (ii) into two or more complexes m. An evolution routine is performed (iii) in which each complex is optimized by a simplex method. The simplex performs three techniques in order of priority: reflection (reflecting the "worst objective" through the centroid of 2 other points in the parameter space), contraction (new point halfway between the worst point and the centroid of the other points), and mutation (random new point for worst point if reflection and contraction are not possible). When the evolution leads to a better objective function, the points are reshuffled (iv) and the m complexes are repartitioned. These steps (iii and iv) are repeated until the objective does not improve any more, or until a maximal number of iterations is reached. The reshuffle reduces the risk that the routine gets stuck in a local minimum. Refer to Duan et al. (*34*) for a comprehensive description of the SCE routine.

The multi-objective minimization problem was solved by the aggregation of two objectives into one measure. To compensate for differences in magnitude and units between the stated objectives, the two objective functions were transformed to a common distance scale (*19*, *36*, *37*). Both objective functions were first normalized and then transformed to have the same distance from the origin to the optimum of the initial sample. The transformation function is given by

$$g_i(F_i) = \frac{F_i}{\sigma_i} + \epsilon_i, \quad i = 1, 2 \tag{10}$$

where F_i is the objective function of the i-th iteration, σ_i is the standard deviation of the i-th iteration (calculated on an initial set of calculations), and ϵ_i is a transformation constant given by (*36*, *37*)

$$\epsilon_i = \max\left\{\min\left\{\frac{F_j}{\sigma_j}\right\}, \quad j = 1,2\right\} - \min\left\{\frac{F_i}{\sigma_i}\right\} \tag{11}$$

The aggregated objective function is given by

$$F_{agg} = \omega\left(\frac{F_1}{\sigma_1} + \epsilon_1\right) + (1 - \omega)\left(\frac{F_2}{\sigma_2} + \epsilon_2\right) \tag{12}$$

where ω is a weighting factor, varying from 0 to 1.

The parameters to be optimized are summarized in Table 3 with the applied constraints. It should be noted that the injection and extraction rates were fixed for all injection and extraction points. The constraints are chosen for computational reasons (too large computational requests when the injection and extraction rates are unrealistically high), technical reasons, or economic concerns (too large remediation time).

For each value of ω, the UTCHEM model was optimized for each pumping well scenario (since the number of wells is a discrete parameter it would not be computationally feasible to optimize it numerically). This resulted in *n_scen* scenario optima of which a global optimum could be derived for that ω-value.

The result of a multi-objective calibration is not a single unique set of parameters but consists of the so-called "Pareto set" of solutions or a "Pareto front" (*19*, *22*). In the simplest case of two objectives as is the case here, points on the Pareto front have the characteristic that no other points have both a smaller value of F_1 and a smaller value of F_2. The Pareto

TABLE 4. Overview of Partial Costs of the Total Cost Function with Their Specification

description	units	cost	specification
fixed cost	euros	50 000	installation pumping group, water purification, etc.
surfactant costs	euros L^{-1}	35.5	cost per liter of surfactant
time costs	euros d^{-1}	240	labor cost, rent of equipment
cost per well	euros	850	cost per additional well
extraction costs	euros m^{-3}	0.25	monitoring, replacement of active coal, energy

TABLE 5. Remediation Variables, Determined through Optimization, Costs, and Remaining DNAPL Saturation, for Different Weighting Factors

ω	extr. rate (m^3 d^{-1})	inj. rate (m^3 d^{-1})	T1 (d)	T2 (d)	scenario	surf. wt frac. (dimensionless)	extr. cost (euros)	time cost (euros)	surf. cost (euros)	well cost (euros)	tot. cost (euros)	fract. sat. (dimensionless)
0.000	4.8	1.9	11.1	14.0	1	0.0007	141	11,500	479	1,700	63,822	1.000
0.125	7.4	2.8	15.0	16.9	1	0.0013	371	13,299	568	1,700	68,298	0.977
0.250	92.0	33.7	17.2	24.3	7	0.0072	7,462	18,572	70,137	15,300	161,472	0.320
0.375	94.9	35.2	21.9	16.6	6	0.0067	6,922	18,434	102,273	15,300	192,929	0.173
0.500	91.2	39.5	22.0	21.9	7	0.0077	8,366	20,681	111,792	15,300	206,140	0.139
0.625	99.3	41.8	31.0	23.4	6	0.0058	10,262	24,657	136,479	15,300	236,698	0.078
0.750	95.4	46.0	34.2	20.4	6	0.0056	10,879	26,044	176,400	15,300	278,624	0.044
0.875	96.1	48.4	51.4	28.6	7	0.0058	16,388	35,811	239,217	15,300	356,716	0.013
1.000	96.9	44.8	67.4	46.0	7	0.0056	25,425	51,673	352,800	15,300	495,199	0.01

front shows a tradeoff between the two different objectives. Important characteristics of the Pareto front are its distance to the axes (absolute values for the two objectives) and its shape (i.e., amount of tradeoff when following the curve toward one unique objective).

In this study, the Pareto front was calculated by performing several sets (using different weights for the objectives $0 \leq \omega \leq 1$) of a series (for each scenario) of SCE optimizations. F_1 evaluates the fraction of average DNAPL saturation (dimensionless, between 0 and 1) left after the remediation; F_2 evaluates the total aggregated cost in euros of the remediation. There is a straightforward tradeoff between these two objectives: a more intensive remediation (higher pumping rates, longer remediation time, more wells, a higher surfactant concentration, etc.) generally reduces the remaining average saturation but boosts the total cost of the remediation and vice versa.

The total cost is an aggregation of partial costs related to different surfactant remediation activities:

$$cost_{tot} = cost_{fix} + cost_{surf} \times mass_{surf} + cost_{time} \times time_{rem} + cost_{well} \times n_{well} + cost_{purif} \times vol_{extr} \quad (13)$$

where the costs are, respectively: the total cost (euros), the fixed cost (euros), related to tests on the surfactant−pollutant mixture and sampling costs, the cost of the surfactant (euros kg^{-1}), the cost per time unity (e.g., labor costs, hiring of material, electricity, etc.) (euros d^{-1}), the cost per extra well (euros/well) (drilling, tubing, filters), and the cost for the purification of the extracted water (replacing of the active coal filters) (euros m^{-3}). An overview of the costs was calculated from former remediations (e.g., 19) and is given in Table 4.

3. Results and Discussion

A large number of UTCHEM simulations were executed to obtain a Pareto set of optima and analyze the tradeoff between total cost and the relative DNAPL removal.

A preliminary test revealed that the SCE algorithm was able to rapidly find a global minimum for the model with three complexes ($m = 3$). This allowed reducing the number of iterations and keeping the problem computationally feasible. In this case, the evaluation of remediation value

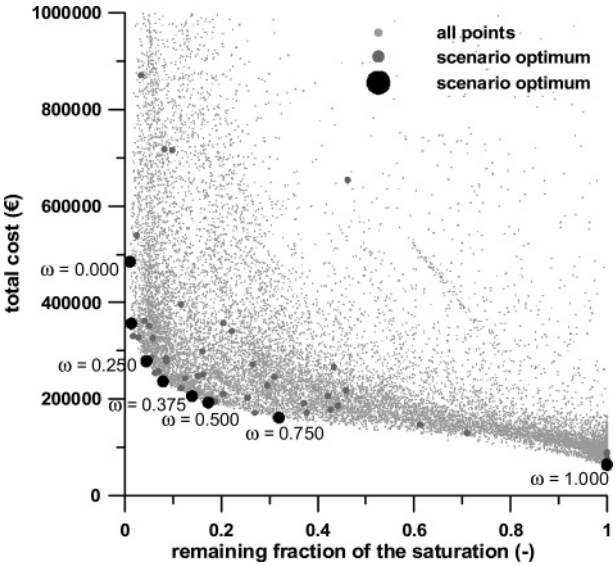

FIGURE 4. Pareto front with all parameter realizations and optima for different values of ω, with ω the weighting factor for the remediation effectiveness.

sets converged after about 150−200 model operations. Optimization was performed for 9 equidistant values ω between 0 and 1 with 280 iterations for each of the 9 pumping well setup scenarios, which means a total of 22 680 simulations. This resulted in 9 calculated scenario optima (see Figure 4) that form a so-called Pareto front. No points were found to the left or under the Pareto curve, which is an indication that the derived optima are global optima.

Inspection of the individual remediation cases showed that the DNAPL was partly mobilized and that an intermediate microemulsion phase was formed. This microemulsion was not observed to sink in the aquifer due to its higher density. The cost range (given the constraints for the input parameters from Table 3) is considerable: 63 000−1 930 000 euros (the *Y*-axis in Figure 4 is limited for reasons of clarity). The fraction remaining DNAPL saturation varies between 1 and 0, i.e., over the complete possible range. The observed Pareto front is rather sharp and asymmetric. The reduction of the first

80% of the DNAPL saturation cost relatively little money. The cost of the removal of the last 20% of the contamination increases steeply. When given no weight to the cost, the DNAPL can be removed completely. On the other hand, no DNAPL at all is removed when no weight was contributed to the remediation effectiveness. The cost consists of the sum of the fixed cost and the minimal constraints of the remediation variables times their associated costs. Remarkably, a large difference in remediation result is noted for $0.750 < \omega < 0.825$.

The remediation variables that were obtained through optimization are summarized in Table 5.

In general, the remediation variables grow with increasing ω (with an increasing weight for the DNAPL removal effectiveness). The fastest increase lies for ω values between 0 and 0.25 for the injection and extraction rates and for ω values between 0.75 and 1 for the pumping duration. The surfactant concentration remains rather constant for all optima where an effective remediation was carried out ($\omega >$ 0.125). For all ω values (except for where almost no DNAPL is removed), the scenarios 6 or 7 seem to be optimal (the two scenarios are very comparable in setup, with a mutual distance between injection and extraction points of 3 m).

All scenarios on the Pareto front are optima, whereas for other setups (to the right or above the Pareto front) an alternative can always be found that is cheaper and/or more effective. From a multi-objective point of view, all the scenarios lying at the Pareto front are equally "good". The selection of a remediation setup on the Pareto front must depend on other criteria external to the multi-objective optimization, e.g., the maximum available budget or the maximum allowed remaining contamination level. The shape of the Pareto curve is strongly dependent on the remediation characteristics (aquifer properties, DNAPL distribution, DNAPL type, selected surfactant), and on the applicable costs (dependent on available equipment, labor costs, etc.). The presented modus operandi allows decision makers to make an optimal choice taking into account their budget and regulatory remediation objectives.

Acknowledgments

J.S. has a postdoctoral scholarship of the Flemish Institute for the Encouragement of Scientific-Technological Research in the Industry (IWT). The University of Texas at Austin is gratefully acknowledged for the use of the UTCHEM simulator. Jan Vanlinden and Gert Vermeiren (URS Belgium) are acknowledged for the information on remediation costs.

Literature Cited

(1) Pankow, J. F.; Cherry, J. A. *Dense Chlorinated Solvents and Other DNAPLs in Groundwater*; Waterloo Press: Portland, OR, 1996.

(2) ITRC. *Dense Nonaqueous Phase Liquids (DNAPLs): Review of Emerging Characterization and Remediation Technologies*; Interstate Technology and Regulatory Cooperation Work Group: Washington, DC, 2000.

(3) Schwille, F. *Dense Chlorinated Solvents in Porous and Fractured Media Model Experiments* (English Language Edition); Lewis Publishers: Chelsea, MI, 1988.

(4) Mackay, D. M.; Cherry, J. A. Groundwater contamination: Pump-and-treat remediation. *Environ. Sci. Technol.* **1989**, *23*, 630.

(5) Brown, C. L.; Delshad, M.; Dwarakanath, V.; McKinney, D. C.; Pope, G. A. *Design of a field-scale surfactant enhanced remediation of a DNAPL contaminated aquifer*; Presented at the I&EC Special Symposium of the American Chemical Society, Birmingham, AL; American Chemical Society: Washington, DC, 1996.

(6) Martino, M. R. Comparison between UTCHEM simulation and the field data from the remediation of a DNAPL contaminatedaquifer at Hill AFB, Utah. U. S. Army Corps of Engineers, Vicksburg, MS, 1999; publication pending.

(7) Istok, J. D.; Field, J. A. *In-situ, field scale evaluation of surfactant-enhanced DNAPL recovery using a single-well, "push−pull" test*. Final report, project 55196-OR; 1999.

(8) U.S. EPA. *In Situ Remediation Technology Status Report: Surfactant Enhancements*; U. S. Environmental Protection Agency, Office of Solid Waste and Emergency Response, Technology Innovation Office: Washington, DC, 1996.

(9) Jafvert, C. T. *Surfactants/Cosolvents*, GWRTAC Series E report; Groundwater Remediation Technology Analysis Center: Pittsburgh, PA, 1996.

(10) Fountain, J. C. *Technologies for Dense Nonaqueous Phase Liquid Source Zone Remediation*; Groundwater Remediation Technologies Analysis Center: Pittsburgh, PA, 1998.

(11) U.S. EPA. *Technical support session meeting*; San Antonio, TX, 1998.

(12) U.S. EPA. *Innovative Remediation Technologies: Field-Scale Demonstration Projects in North America*, 2nd ed., Year 2000 Report (542-B-00-004); Office of Solid Waste and Emergency Response, U.S. Environmental Protection Agency: Washington, DC, 2000.

(13) Strbak, L. *In Situ Flushing with Surfactants and Cosolvents*; U.S. EPA, Washington DC, 2000; 31 p.

(14) ITRC. *Dense Nonaqueous Phase Liquids (DNAPLs): Review of Emerging Characterization and Remediation Technologies*; Interstate Technology and Regulatory Cooperation Work Group: Washington, DC, 2000.

(15) Stundner, M.; Zangl, G. Einsatzmöglichkeiten von biologisch abbaubaren Tensiden zur Bodenund Grundwassersanierung am Beispiel des Produktes "BioVersal" unter besonderer Berücksichtigung der Standortverhältnisse in der Stadt Wien, 2000; 89 p.

(16) ESTCP. Cost and Performance Report: Surfactant Enhanced DNAPL Removal; Environmental Security Technology Certification Program, U.S. Department of Defense: 2001.

(17) Duke Engineering Services. Final Cost and Performance Report for Surfactant-Enhanced DNAPL Removal at site 88, Marine Corps Base, Camp Lejeune, North Carolina; Charlotte, NC, 2001; 104 p.

(18) Field, J. A.; Sawyer, T. E.; Schroth, M. H.; Humphrey, M. D.; Istok, J. D. Effect of cation exchange on surfactant-enhanced solubilization of trichloroethene. *J. Contam. Hydrol.* **2000**, *46*, 131.

(19) Schaerlaekens, J.; Mertens, J.; Van Linden, J.; Vermeiren, G.; Carmeliet, J.; Feyen, J. A multi-objective optimization framework for surfactant-enhanced remediation of DNAPL contaminations. *J. Contam. Hydrol.*; submitted for publication.

(20) Schaerlaekens, J.; Feyen, J. Effect of scale and dimensionality on the surfactant-enhanced solubilization of a residual DNAPL contamination. *J. Contam. Hydrol.* **2004**, *71*, 283.

(21) Mayer, A. S.; Kelley, C. T.; Miller, C. T. Optimal design for problems involving flow and transport phenomena in saturated subsurface systems. *Adv. Water Resour.* **2002**, *25*, 1233.

(22) Pareto, V. *Manual of Political Economy*; orig. 1906 in Italian; 1927 in French; 1971 translated by Ann S. Schwier; Augustus M. Kelley: New York, 1971.

(23) Center for Petroleum and Geosystems Engineering, University of Texas at Austin. *UTCHEM 9.0 Volume I. Users Guide*. Austin, TX, 2000.

(24) Pope, G. A.; Nelson, R. C. A Chemical Flooding Compositional Simulator. *Soc. Pet. Eng. J.* **1978**, *18*, 339.

(25) Delshad, M.; Pope, G. A.; Sepehrnoori, K. A compositional simulator for modeling surfactant-enhanced aquifer remediation, 1 Formulation. *J. Contam. Hydrol.* **1996**, *23*, 303.

(26) Pennell, K. D.; Pope, G. A.; Abriola, L. M. Influence of viscous and buoancy forces on the mobilization of residual tetrachloroethylene during surfactant flushing. *Environ. Sci. Technol.* **1996**, *30*, 1328.

(27) Huh, C. Interfacial tension and solubilizing ability of a microemulsion phase that coexists with oil and brine. *J. Colloid Interface Sci.* **1979**, *71*, 408.

(28) Hirasaki, G. J. Application of the theory of multicomponent, multiphase displacement to three-component, two-phase surfactant flooding. *Soc. Pet. Eng. J.* **1981**, 191.

(29) Dekker, T. J.; Abriola, L. M. The influence of field-scale heterogeneity on the surfactant-enhanced remediation of entrapped nonaqueous phase liquids. *J. Contam. Hydrol.* **2000**, *42*, 187.

(30) Kraichnan, R. H. Dynamics of Nonlinear Stochastic Systems. *J. Math. Phys.* **1961**, *2*, 124−148.

(31) Woodbury, A. D.; Sudicky, E. A. Inversion of the Borden tracer experiment data: Investigation of stochastic moment models.*Water Resour. Res.* **1991**, *27*, 533.

(32) Hoag, G. E.; Marley, M. C. Gasoline residual saturation in unsaturated uniform aquifer materials. *J. Environ. Eng.* **1986**, *112*, 586.

(33) Larson, R. G.; Davis, H. T.; Scriven, L. E. Percolation theory of 2-phase flow in porous media. *Chem. Eng. Sci.* **1981**, *36*, 75.

(34) Duan, Q.; Sorooshian; S.; Gupta, V. K. Effective and efficient global optimisation for conceptual rainfall-runoff models. *Water Resour. Res.* **1992**, *28*, 1015.

(35) Duan, Q.; Sorooshian, S.; Gupta, V. K. Optimal use of the SEC−UA global optimisation method for calibrating watershed models. *J. Hydrol.* **1994**, *158*, 265.

(36) Madsen, H. Parameter estimation in distributed hydrological catchment modelling using automatic calibration with multiple objectives. *Adv. Water Resour.* **2003**, *26*, 205.

(37) Mertens, J.; Madsen, H.; Feyen, L.; Jacques, D.; Feyen, J. Including prior information in the estimation of effective soil parameters in unsaturated zone modeling. *J. Hydrol.* **2004**, *294*, 251.

Received for review June 7, 2004. Revised manuscript received December 22, 2004. Accepted January 3, 2005.

ES049148Z